J Bionic Eng 17 (2020) 944–958
DOI: https://doi.org/10.1007/s42235-020-0079-3

Journal of Bionic Engineering
http://www.springer.com/journal/42235

Path Optimization Method for the Spherical Underwater Robot in Unknown Environment

Jian Guo[1], Chunying Li[1,2], Shuxiang Guo[1,2*]

1. *Tianjin Key Laboratory for Control Theory & Applications in Complicated Systems and Intelligent Robot Laboratory*, *Tianjin University of Technology*, *Tianjin* 300384, *China*
2. *Department of Intelligent Mechanical Systems Engineering*, *Faculty of Engineering*, *Kagawa University*, *Takamatsu* 761-0396, *Japan*

Abstract

One of the major respects of the autonomous capability of underwater robots in unknown environment is to be capable of global path planning and obstacles avoiding when encountering abrupt events. For the Spherical Underwater Robot (SUR) to fulfill autonomous task execution, this paper proposed a novel fuzzy control method that incorporates multi-sensor technology to guide underwater robots in unknown environment. To attain the objective, a SUR we designed is used to design the controller. According to its kinematic model, the safety distance was calculated and sensors (US1000-21A) were arranged. The novel fuzzy control method was then explored for robot's path planning in an unknown environment through simulation. The simulation results demonstrate the capability of the proposed method to guide the robot, and to generate a safe and smooth trajectory in an unknown environment. The effectiveness of the proposed method was further verified through experiments with a SUR in a real platform. The real environment experiments by using the novel fuzzy control method were compared with the basic control method. The experimental results show that in unknown environments, the proposed method improves the execution efficiency and flexibility of the SUR.

Keywords: path planning, fuzzy control, spherical underwater robot, unknown environment

1 Introduction

Currently, the path planning and autonomous navigation of underwater robots have been widely used in water patrol, military reconnaissance, and pipeline inspection scenarios[1,2]. However, most environments are dynamic and unknown when the robot is performing tasks, and the mathematical model of the robot cannot be accurately constructed[3,4]. This paper, therefore, attempts to improve the efficiency and stability of the Spherical Underwater Robot (SUR) we designed to work in unknown environments. Based on the multi-sensor technology and kinematic model of the SUR, a novel fuzzy control method is proposed.

In recent years, many researches have been carried out on path planning, which is becoming a hot topic in the field of robotics[5,6]. Ma *et al*. proposed a path planning method based on the ant colony algorithm[7], which combines multi-constrained features, but does not consider the unknown environments. Duan *et al*. proposed a real-time path planning method for AUV based on fuzzy control[8,9], and the detection range of the sensor is limited. Chen *et al*. studied the path tracking problem of underwater robots under different conditions[10,11], but lacking consideration of constraints.

Although numerous achievements have been made in path planning and navigation of underwater robot, the research remains inadequate for many practical works. The first reason is that most underwater robots are nonlinear systems, and it is difficult to build accurate mathematical models[12]. The second reason is the lack of consideration of multi-sensor technology to meet the needs of tasks in unknown environments. Therefore, this paper proposes a novel fuzzy control method that does not rely on accurate mathematical models and has the strong anti-interference ability.

To implement the autonomous navigation capability of the SUR, in previous works, we designed a control system for the SUR[13,14], which realized the switching of multiple behaviors of the robot. We also designed a

***Corresponding author:** Shuxiang Guo
E-mail: 27929579@qq.com

multi-robot collaborative control system, which achieved coordination between multiple robots[15]. In the present paper, based on these control strategies, we focus on the path planning of the SUR in unknown environments[16]. And the effectiveness and feasibility of the proposed method are verified by simulations and experiments. Our contributions are:

Due to the limited detection distance of the sensors and the uncertainty of the surrounding environments, this paper uses multi-sensor technology to implement the autonomous navigation capability of the SUR in an unknown environment. Next, obstacle avoidance of the SUR plays an important role in path planning. Therefore, this paper improves the self-adjust ability of the SUR by solving the parameters of the end effector of the water jet. Then, in this paper, path planning experiments of the SUR in unknown and moving obstacle environments are performed. Simulation and experimental results show that the proposed method effectively improves the performance of the SUR.

The paper is organized as follows: First, we propose a novel fuzzy control method, and describe the feasibility results from several previous works. Then, the second part introduces the research strategy of SUR path planning, and the minimum safety distance is obtained according to the robot model, and the sensor arrangement is executed. Next, in section **3**, the design of the fuzzy controller and the simulation experiments in an unknown environment is designed. Next, section **4** uses the SUR to carry out the path planning experiments in an unknown environment. And section **5** discusses some underwater experiments. Finally, section **6** presents our conclusions.

2 Methodology

2.1 Motion model of the SUR

During underwater motion, the essence of SUR path planning is the inverse solution of position. Taking the horizontal motion of the SUR as an example, the solution of the horizontal motion equation is obtained in this paper[17–19].

The horizontal motion of the SUR is mainly described by the forward velocity μ, the lateral velocity v, and the heading angle r. The coordinate vector is defined as $\boldsymbol{\eta}_h = [\boldsymbol{\xi}\ \boldsymbol{\eta}\ \boldsymbol{\psi}]^{\mathrm{T}}$, where $\boldsymbol{\xi}$, $\boldsymbol{\eta}$ and $\boldsymbol{\psi}$ are the Euler angle of horizontal plane movement; the velocity vector is defined as $\boldsymbol{V}_h = [\boldsymbol{\mu}\ \boldsymbol{v}\ \boldsymbol{r}]^{\mathrm{T}}$. In this paper, the off-diagonal terms of the inertia matrix and the damping matrix in the dynamic model are ignored, and the equation of Horizontal plane motion is obtained as shown in Eqs. (1) and (2).

$$\dot{\boldsymbol{\eta}}_h = \boldsymbol{R}_h(\psi)\boldsymbol{V}_h, \tag{1}$$

$$\boldsymbol{M}_h\dot{\boldsymbol{V}}_h + \boldsymbol{C}_h(\boldsymbol{V}_h)\boldsymbol{V}_h + \boldsymbol{D}_h(\boldsymbol{V}_h)\boldsymbol{V}_h = \boldsymbol{\tau}_h, \tag{2}$$

where $\boldsymbol{R}_h(\psi)$ is the transformation matrix of the SUR, as shown in Eq. (3); $\boldsymbol{M}_h$ is the inertia matrix of the SUR, as shown in Eq. (4); $\boldsymbol{C}_h(\boldsymbol{V}_h)$ is the Coriolis force and the centripetal force matrix, as shown in Eq. (5); $\boldsymbol{D}_h(\boldsymbol{V}_h)$ is the damping matrix, as shown in Eq. (6); $\boldsymbol{\tau}_h$ is the force generated by the actuator of the SUR, as shown in Eq. (7).

$$\boldsymbol{R}_h(\psi) = \begin{bmatrix} \cos\psi & \sin\psi & 0 \\ -\sin\psi & \cos\psi & 0 \\ 0 & 0 & 1 \end{bmatrix}, \tag{3}$$

$$\boldsymbol{M}_h = \begin{bmatrix} m - X_{\dot{u}} & 0 & 0 \\ 0 & m - Y_{\dot{v}} & 0 \\ 0 & 0 & I_z - N_{\dot{r}} \end{bmatrix}, \tag{4}$$

$$\boldsymbol{C}_h\left(\boldsymbol{V}_h\right) = \begin{bmatrix} 0 & 0 & -\left(m - Y_{\dot{v}}\right)v \\ 0 & 0 & \left(m - X_{\dot{u}}\right)u \\ \left(m - Y_{\dot{v}}\right)v & -\left(m - X_{\dot{u}}\right)u & 0 \end{bmatrix}, \tag{5}$$

$$\boldsymbol{D}_h\left(\boldsymbol{V}_h\right) = \begin{bmatrix} -X_u & 0 & 0 \\ 0 & -Y_v & 0 \\ 0 & 0 & -N_r \end{bmatrix} + \begin{bmatrix} -X_{u|u|} & 0 & 0 \\ 0 & -Y_{v|v|} & 0 \\ 0 & 0 & -N_{r|r|}|r| \end{bmatrix}, \tag{6}$$

$$\boldsymbol{\tau}_h = [X\ Y\ N]^{\mathrm{T}}. \tag{7}$$

Substituting the parameters (Eq. (3) to Eq. (7)) into Eqs. (1) and (2) to obtain the horizontal kinematic equation of the SUR, as shown in Eq. (8).

$$\begin{cases} (m - X_{\dot{u}})\dot{\boldsymbol{u}} = \left(m - Y_{\dot{v}}\right)vr + \left(X_u + X_{u|u|}|u|\right)u + X \\ (m - Y_{\dot{v}})\dot{\boldsymbol{v}} = -(m - X_{\dot{u}})ur + \left(Y_v + Y_{v|v|}|v|\right)v \\ \left(I_z - N_{\dot{r}}\right)\dot{\boldsymbol{r}} = -\left(X_{\dot{u}} - Y_{\dot{v}}\right)uv + (N_r + N_{r|r|}|r|)r + N \end{cases}. \tag{8}$$

2.2 S-function of the SUR

After analyzing the kinematic equation of the SUR, this paper obtained the model parameters of the SUR. The total mass M of the SUR is shown in Eq. (9)[20].

$$M = M_R + M_A, \tag{9}$$

where M_A is the additional mass parameter, as shown in Eq. (10). M_R is the inertial mass parameter, as shown in Eq. (11). The damping coefficient D_V is shown in Eq. (12).

$$\begin{aligned} M_A &= diag\left\{X_{\dot{u}}, Y_{\dot{v}}, Z_{\dot{w}}, K_{\dot{p}}, M_{\dot{q}}, N_{\dot{r}}\right\} \\ &= diag\left\{4.09, 4.09, 4.09, 0, 0.0554, 0.0629\right\}, \end{aligned} \tag{10}$$

$$\begin{aligned} M_R &= diag\left\{m, m, m, I_x, I_y, I_z\right\} \\ &= diag\left\{3.58, 3.58, 3.58, 0, 0, 0.0075\right\}, \end{aligned} \tag{11}$$

$$\begin{aligned} D(V) &= diag\left\{X_u, Y_v, Z_w, K_p, M_q, N_r\right\} \\ &= diag\left\{9.78, 9.78, 9.78, 1.22, 1.22, 1.22\right\}. \end{aligned} \tag{12}$$

After the model parameters are determined, this paper uses Matlab to write the S-function of the SUR, as shown in Table 1. The Parameters of additional mass coefficient $X_{\dot{u}}, Y_{\dot{v}}, Z_{\dot{r}}$, as shown in Eq. (10); The parameters of inertial mass coefficient m and I_x, as shown in Eq. (11). The parameter of damping coefficient X_μ, Y_v and Z_r, as shown in Eq. (12).

Table 1 S-function of the SUR

	Algorithm 1 SUR-S-function
1:	function [$\dot{u}$, $\dot{v}$, $\dot{r}$, $\dot{\xi}$, $\dot{\eta}$, $\dot{\psi}$] = fcn(u, v, w, X, N, ξ, η, ψ)
2:	/*Initial Definition*/
3:	**/*Parameters of inertial mass coefficient*/**
4:	$m = 3.58$;
5:	$I\_z = 0.0075$;
6:	**/*Parameters of additional mass coefficient*/**
7:	$X\_\dot{u} = -4.09$;
8:	$Y\_\dot{v} = -4.09$;
9:	$N\_\dot{r} = -4.09$;
10:	/***Parameter of damping coefficient***/
11:	$X\_u = -9.78$;
12:	$Y\_v = -9.78$;
13:	$N\_r = -9.78$;
14:	$X\_uu = -0$;
15:	$Y\_vv = -0$;
16:	$N\_rr = -0$;
17:	/*Main Function*/
18:	**/*The horizontal dynamic and kinematics equations of the**
19:	**SUR*/**
20:	$\dot{u} = ((m - Y\_\dot{v})\cdot v\cdot r + (X\_u + X\_uu\cdot abs(u))\cdot u + X)/(m - X\_\dot{u})$;
21:	$\dot{v} = (-(m - X\_\dot{u})\cdot u\cdot r + (Y\_v + Y\_vv\cdot abs(v))\cdot v)/(m - Y\_\dot{v})$;
22:	$\dot{r} = (-(X\_\dot{u} - Y\_\dot{v})\cdot u\cdot v + (N\_r + N\_rr\cdot abs(r))\cdot + N)/(I\_z - N\_\dot{r})$;
23:	$\dot{\xi} = u\cdot\cos(\psi) - v\cdot\sin(\psi)$;
24:	$\dot{\eta} = u\cdot\sin(\psi) + v\cdot\cos(\psi)$;
25:	$\dot{\psi} = r$;

2.3 Ultrasonic sensor US1000-21A layout and optimization

This paper uses multi-sensor fusion technology to improve the obstacle avoidance ability of spherical underwater robots in unknown environments[21–23]. The US1000-21A ultrasonic sensor module is used to complete the path planning of the SUR. According to the motion characteristics of the SUR and the ranging principle of the ultrasonic sensor, this paper designs the overall mechanical structure of the SUR, as shown in Fig. 1. A total of four ultrasonic sensors are arranged, and the two sides of the sensors are symmetrical.

The SUR detects the distance from the surrounding obstacles by the ultrasonic sensors fixed on the robot. The angle between the front-left ultrasonic sensor and the central axis is 30°, as is the front-right ultrasonic sensor, as shown in Fig. 1b.

The arrangement of the ultrasonic sensors is determined based on the safety distance of the SUR. This paper uses multi-sensor fusion technology to optimize the path planning of SUR. A total of four ultrasonic sensors are used. The schematic diagram of obstacle detection by the left and right sensors is shown in Fig. 2, where $L1$ and $L2$ represent the left-sensors, $R1$ and $R2$ represent the right-sensors. According to the distribution of obstacles, the SUR movement can be divided into three situations: forward, leftward and rightward, respectively. In order to obtain the minimum safety distance of the SUR, the center of the SUR is set as a reference point, the motion of the SUR can be regarded as circular motion, wherein the linear motion is the motion when the radius of the arc is infinite. The SUR has a certain time interval, generally 100 ms, when reading the sensor information. Therefore, when the SUR has a large speed, the time lag distance must be considered. The maximum moving speed of the SUR used in this paper is 10 cm·s^{-1}, and the time lag distance is at least 1.5 cm.

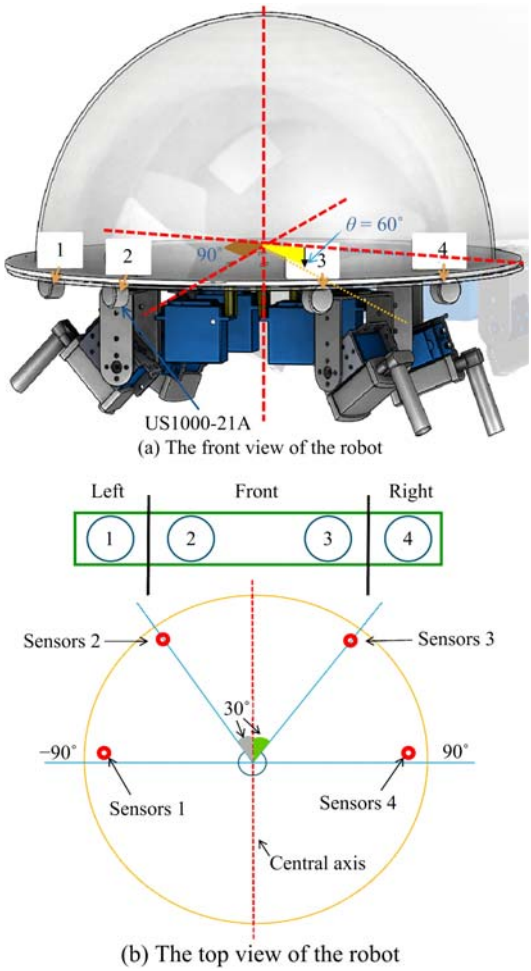

Fig. 1 Overall mechanical structure of the SUR.

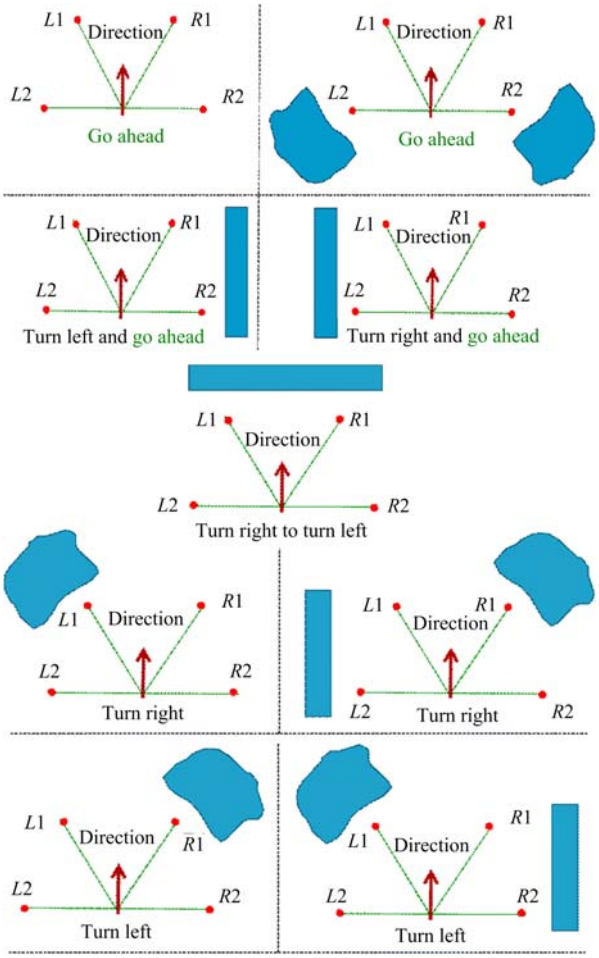

Fig. 2 Obstacle avoidance diagram of the SUR.

The SUR must keep a certain distance from the surrounding obstacles during the path planning process. In order to make the SUR successfully complete the path planning, the minimum safety distance of the SUR is obtained in this paper, as shown in Eq. (13).

$$D = R + R_r, \tag{13}$$

where R is the radius of motion of the robot and R_r is the radius of the SUR.

Next, this paper will calculate the minimum safety distance of the SUR in the following two cases. The first case: When an obstacle is detected in front, the SUR needs to deflect a certain angle (circle motion) to avoid the obstacle. Assume that the movement speed of the SUR is v, the radius of the circular motion is R, and the rotation angle is 90˚, as shown in Fig. 3. The minimum safety distance can be obtained by Eq. (13).

It can be seen from Fig. 3 that the radius R of the circular motion depends on the moving speed v of the

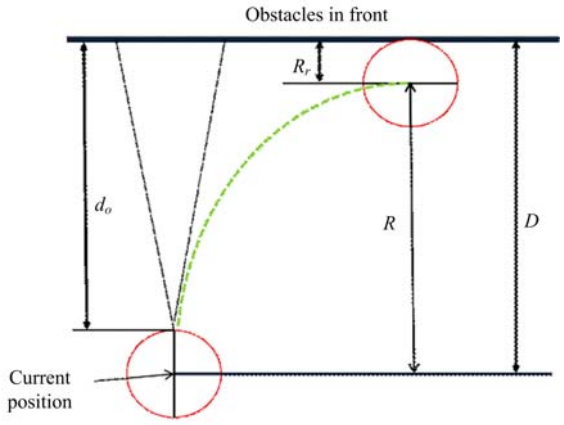

Fig. 3 Minimum safety distance for the SUR with obstacles moving obstacles ahead.

SUR. When the speed v is larger, the radius R is smaller. Since the maximum speed of the SUR is 10 cm·s^{-1}, the radius $R \geq 15.8$ cm can be obtained by the least square method. The distribution radius of the ultrasonic sensors in the SUR is 15.5 cm, so the actual minimum safe distance is $D \geq 15.8 + 15.5 = 31.3$ cm, that is, d_o is about 15.8 cm.

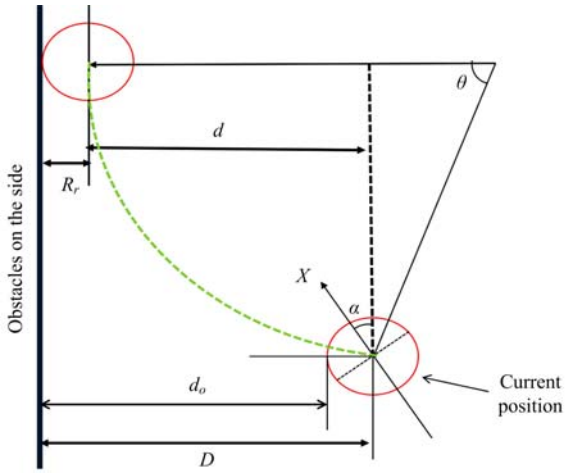

Fig. 4 Minimum safety distance for the SUR with obstacles on the side (*e.g.* left)

The second case: When an obstacle is detected on the side, for example, on the left, as shown in Fig. 4.

In Fig. 4, α is the angle between the direction of movement and the ordinate of the global coordinate system. Assuming that the SUR makes a circular motion, the minimum safety distance can be obtained from Eq. (14).

$$\begin{aligned} D &= d + R_r = R - R\times\cos\theta + R_r \\ &= R(1-\cos\theta) + R_r \geq 15.8(1-\cos\theta) + 15.5. \end{aligned} \tag{14}$$

3 Models and simulation experiments

3.1 Design of fuzzy controller for the SUR

The SUR detects the distance of the obstacle through ultrasonic sensor (US1000-21A). A total of four ultrasonic sensors are arranged in this paper, which are divided into two groups. In each group, the smaller detection distance is used as the input of the fuzzy controller, that is, min (D_{L1}, D_{L2}) and min (D_{R1}, D_{R2}). Where D_{L1} is the left distance, D_{L2} is the front-left distance, D_{R1} is the front-right distance, and D_{R2} is right distance. The input variable angle α is the angle between the target position and the robot position. The output variables are the rotation angle (θ) and the motion step (S_a).

The membership function is determined by the linearization method, as shown in Eq. (15). The domain of distance d is [0 cm, 80 cm], which is described by three linguistic variables: near (ND), middle (MD), and far (FD). The domain of angle α is [−90°, 90°], which is described by three linguistic variables: left (TL), front (TF), and right (TR). The domain of the rotation angle θ of the SUR is [−90°, 90°], which is described by the language variables NL, NS, Z, PS, and PL. The domain of motion step S_a is [0, 6], which is described by linguistic variables VS, V, and VF.

$$x = k_1 x^* - 10. \tag{15}$$

In Eq. (15), x^* represents the actual distance, x is the range of discrete points, and k_1 represents the scale factor.

The membership function shape of this paper is the symmetrical triangle. Defines that α is positive when the target is in front of the robot, and negative otherwise. When the obstacle is on the right side of the SUR, the membership function of the input variable distance d and angle α are shown in Fig. 5a. And the membership function of the output variable rotation angle θ and motion step S_a are shown in Fig. 5b.

The path planning of the SUR actually adjusts the robot's motion according to the position of the obstacle and target until it reaches the target position. The obstacle avoidance principle is as follows: When multiple obstacles are detected, the one with the smallest distance is selected as the input. When the distance to the obstacle is closer, the speed of the robot is slower. When the distance is longer, the speed of the robot is faster. Fuzzy rules are described in the form of IF-THEN, as shown in Eq. (16).

$$R_i\text{: if } (d_i \text{ is ND and } \alpha \text{ is TL}) \text{ then } (\theta \text{ is NL and } S_a \text{ is VF}). \tag{16}$$

The table of fuzzy control rules is shown in Table 2, where U represents the output variable, that is, the rotation angle θ and motion step S_a.

The fuzzy rule is a matrix that reflects the relationship between input variables and output variables, which can ensure that the robot can avoid obstacles safely and reach the target position smoothly. Next, this paper uses Mamdani's reasoning method to obtain reasoning results, as shown in Fig. 6. The value relationship between variables can be obtained.

This paper uses the center of gravity method for defuzzification, as shown in Eq. (17), which has the characteristics of strong rationality and high accuracy[24,25].

$$Z_0 = \frac{\int z\cdot\mu_N(z)\,dz}{\int \mu_N(z)\,dz}. \tag{17}$$

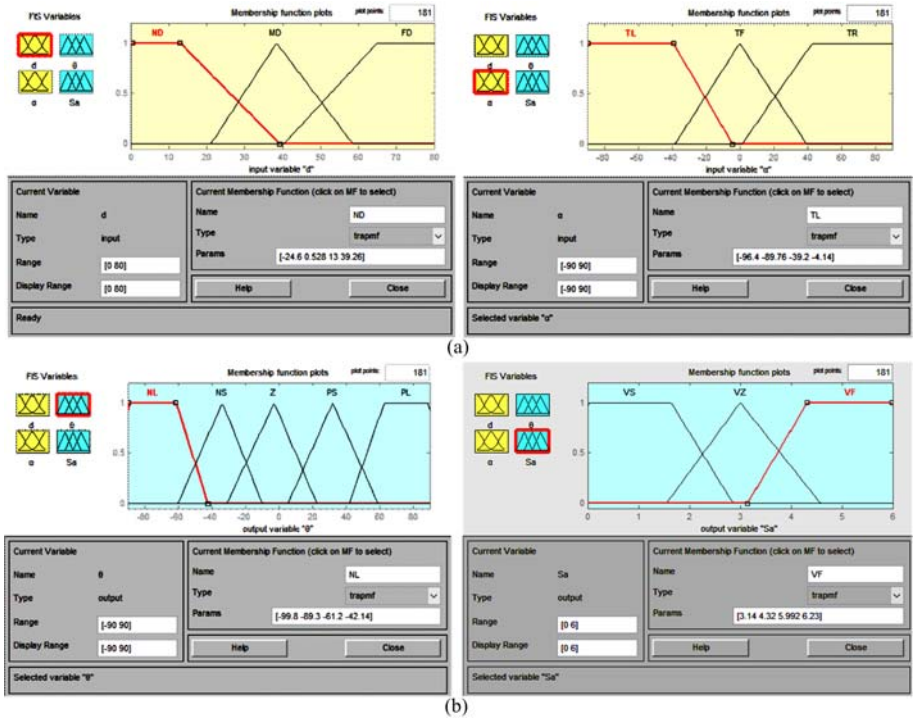

Fig. 5 Membership function of input and output variables of the SUR. (a) Membership function of the input variable distance d (left) and angle α (right); (b) membership function of the output variable corner θ (left) and step size S_a (right).

Table 2 Fuzzy control rule table

D_L / U / a	ND	MD	FD	D_R / U / a	ND	MD	FD
TL	^{R1}[PS, VZ]	^{R4}[NS, VS]	^{R7}[NL, VF]	TL	^{R1}[PL, VF]	^{R4}[PS, VS]	^{R7}[NS, VS]
TF	^{R2}[Z, VS]	^{R5}[Z, VF]	^{R8}[Z, VF]	TF	^{R2}[Z, VS]	^{R5}[Z, VF]	^{R8}[Z, VF]
TR	^{R3}[PL, VF]	^{R6}[PS, VS]	^{R9}[PS, VS]	TR	^{R3}[PS, VZ]	^{R6}[NS, VS]	^{R9}[PL, VF]

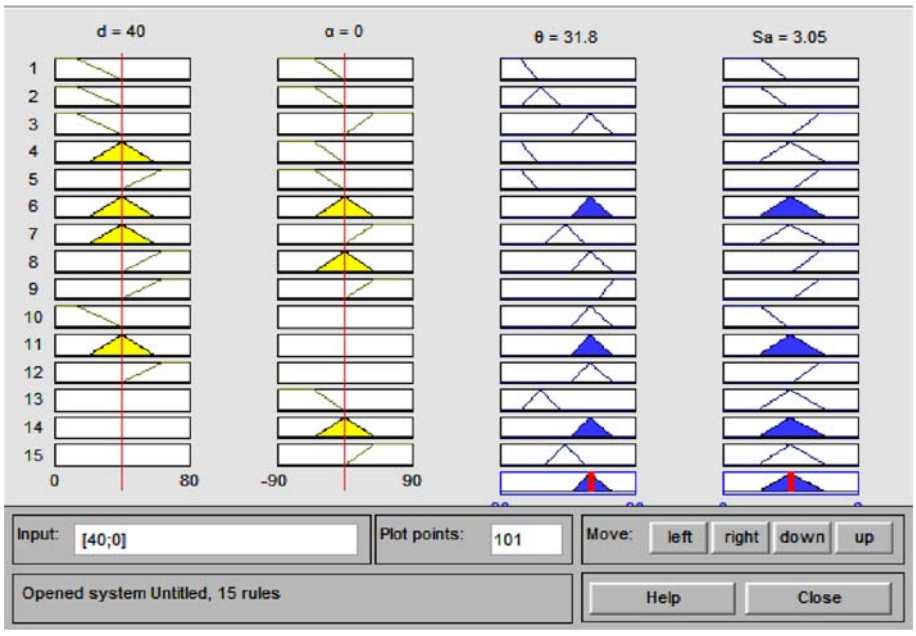

Fig. 6 The result of the fuzzy reasoning.

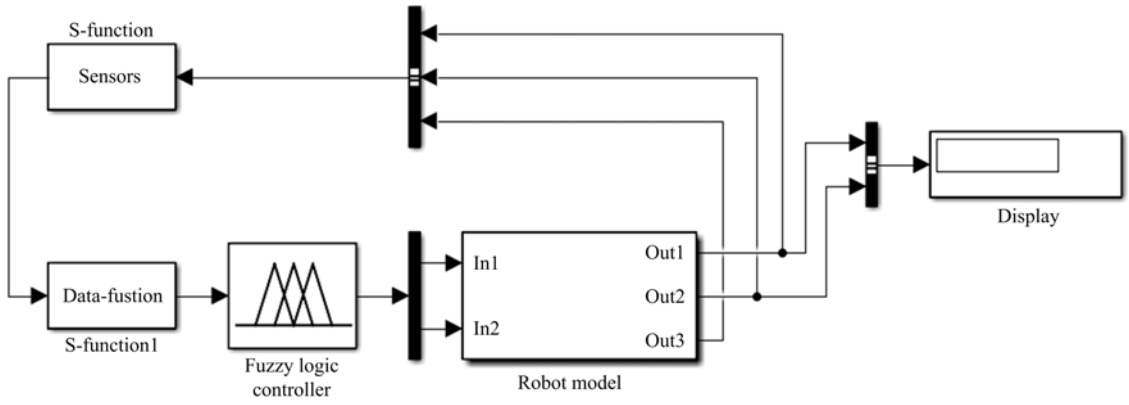

Fig. 7 Fuzzy control simulation model for the SUR.

In Eq. (7), $\int$ represents the integral of all membership values on the continuous domain, $\mu_N(z)$ represents the membership function of the input variable, and z represents the center of gravity of the membership function of the output variable. The purpose of using the center of gravity method is to convert blur amount into the exact amount that is convenient for controlling the movement of the SUR, thereby achieving path planning.

3.2 Simulation experiments in unknown environment

In order to improve the obstacle avoidance performance of the SUR, this paper adds its motion model to the control system and realizes it by S-function (Table 1). The simulation model is designed as shown in Fig. 7, including the fuzzy controller, motion model, multi-sensor obstacle avoidance model, *etc*.

After setting the sampling time and simulation parameters, the simulation experiments of the SUR in an unknown environment are completed, as shown in Fig. 8. To verify the effectiveness and practicability of the fuzzy control algorithm, the comparison experiments are set as follows: By changing the number of obstacles and the position of the target, the number of obstacles is set to 20 (in Fig. 8a), and the number of obstacles is set to 30 (in Fig. 8b).

Among them, the red curve represents the trajectory of the SUR, and the blue represents the obstacles. From the simulation diagram, it can be clearly seen that the robot can effectively avoid the obstacles reaching the target point in real-time under the premise of not colliding with obstacles, and the trajectory is short, which has better effect. By changing the number of obstacles and the state of the target position, the fuzzy control algorithm in the unknown environment has a better obstacle avoidance performance can be effectively verified.

In order to more realistically simulate the experimental environment, this paper uses the fuzzy control method to design state-based path planning experiments. The parameters of the SUR were set through the MOBOTSIM software platform, including the sensor distribution angle, detection range, and the number of sensors, *etc*. The set as follows: the number of sensors is 4, the detection range is 0.8 m, the sensor interval of the left is 60 degrees, and the right too.

According to the obstacle avoidance principle of the SUR, this paper uses the MOBOTSIM platform to complete the path planning experiments when there are obstacles in front and sides of the robot. Among them, the target position is indicated by the yellow circle, and the moving obstacle is indicated by the pink robot.

The path planning experiment when there is a moving obstacle in front of the robot is shown in Fig. 9. Each group of experiments is tested three times. The starting position and the target position were kept consistent during the experiments. Among them, the path planning experiment of the basic control method is shown in Fig. 9a. After using the novel fuzzy control method, as shown in Fig. 9b. It can be seen from Fig. 9 that the robot trajectory is smoother and stable, and the robot can safely reach the target position.

In order to further verify the effectiveness of the novel fuzzy control method, then, this paper carries out the path planning experiment when there is an obstacle on the side, as shown in Fig. 10. The angle between the

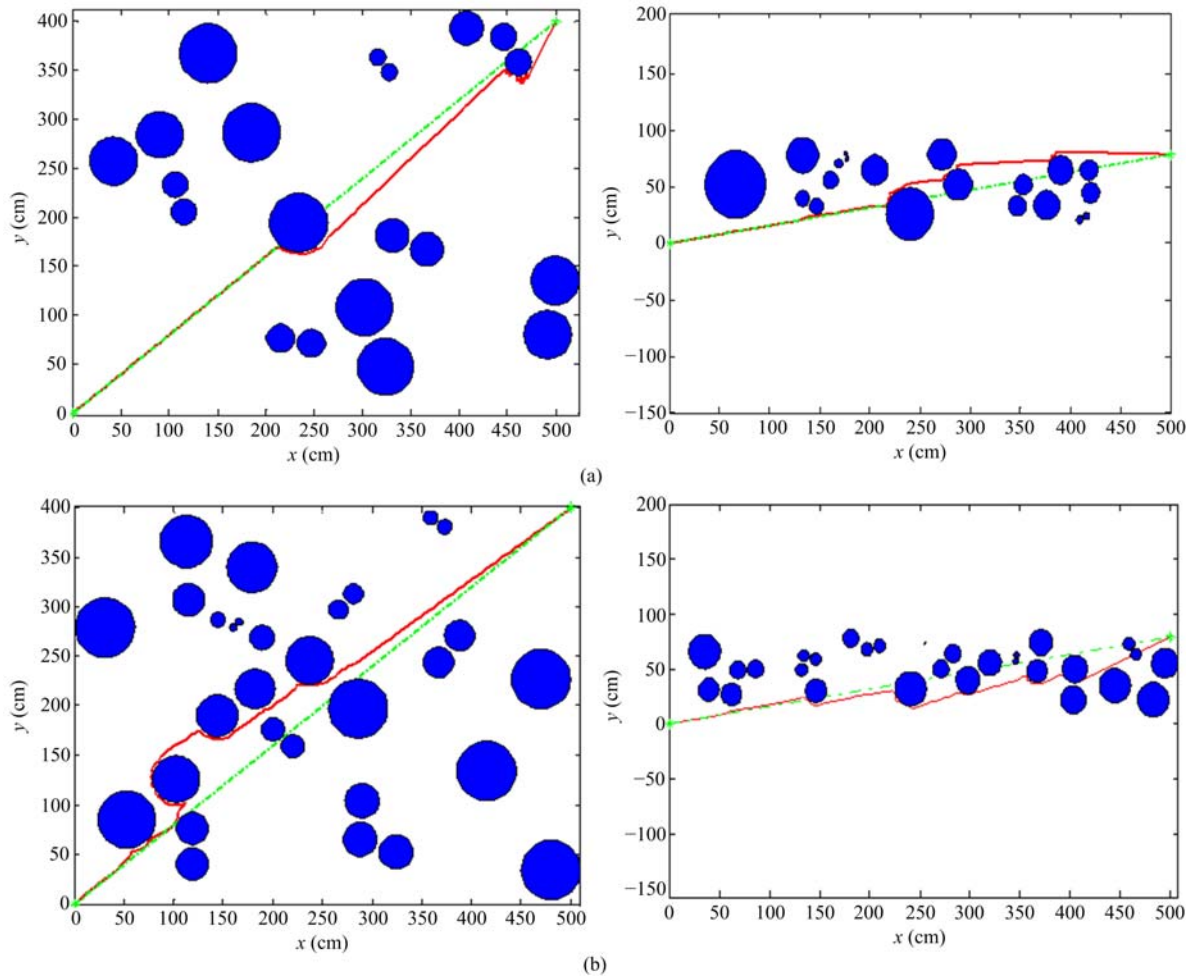

Fig. 8 Simulation results of fuzzy control algorithm in unknown environments. (a) The number of obstacles is 20, and the simulation result of changing the target position; (b) the number of obstacles is 30, and the simulation result of changing the target position.

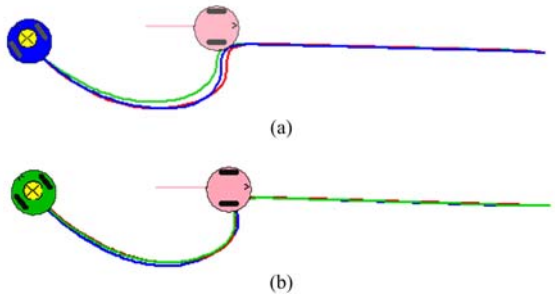

Fig. 9 Simulation path planning experiments of relative motion between robot and obstacle. (a) Experiments with basic control method; (b) experiments with novel fuzzy control method.

target position and the starting position is 45˚. The moving obstacle (pink robot) is located to the right of the master robot. It can be seen from the Fig. 10b that after using the novel fuzzy control method, the movement of the master robot is more stable, and the experimental error is reduced.

4 Experimental results

Most obstacles in the underwater environment are moving, so obstacle avoidance for stationary obstacles is difficult to verify the effectiveness and stability of robot movement. According to the obstacle avoidance model of the SUR, the underwater test is divided into two kinds of environments, the first test: Underwater path planning analysis under the environment of the moving obstacle in front. Second: Underwater path planning analysis under the environment of the moving obstacle on the side.

Firstly, the underwater experimental platform that is 2500 mm in length, 2000 mm in width, and 900 mm in height, the water depth is 600 mm is built, as shown in Fig. 11. Among them, the NDI tracking system tracks the trajectory of the SUR through the passive rigid body

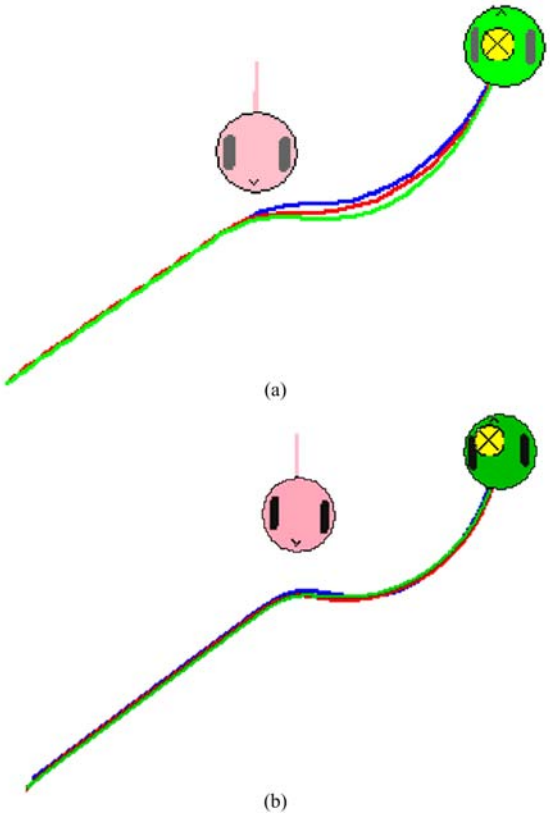

Fig. 10 Simulation path planning experiments with obstacle on the side. (a) Experiments with basic control method; (b) experiments with novel fuzzy control method.

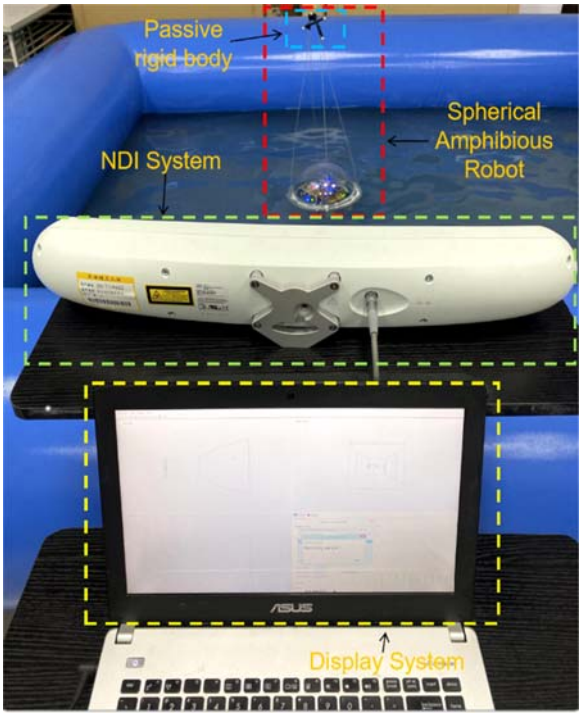

Fig. 11 Experimental set up for underwater path planning experiments.

fixed on the robot. Then, the underwater path planning experiments of the SUR are carried out, including path planning experiments using the fuzzy control method and path planning experiments with basic control method. And the experimental results are analyzed which further verify the effectiveness and feasibility of the fuzzy control method.

4.1 Path planning experiments with moving obstacle ahead

In this experiment, two SURs were used. One SUR was used as the attached robot (Moving Obstacle), and one SUR was used as the master robot for underwater path planning experiments.

In order to verify the obstacle avoidance ability and stability of the SUR with moving obstacle ahead, this paper sets as follows: The attached robot is located in front of the master robot, and the attached robot moves in a straight line. The target position of the master robot and the attached robot are in a straight line to ensure that the master robot continues to move toward the target position after avoiding the obstacle. The movement process of the master robot is shown in Fig. 12. When the robot detects no obstacle, in Fig. 12a, it tends to dominate the target behavior. When the obstacle is detected, in Figs. 12b and 12c), the master robot is dominated by obstacle avoidance behavior. In Figs. 12d–12f, the master robot will continue to move toward the target position after avoiding the obstacle until it reaches the target position.

The trajectory of the master robot is shown in Fig. 13. This paper compares the two group experiments using the fuzzy control method and basic control method. The data is collected by the NDI system, and the starting position and target position of each group of experiments are consistent. Each group of experiments is tested three times.

It can be seen from the trajectory that after the fuzzy control method is adopted, the detection distance of the master robot to the moving obstacle becomes smaller, the distance detection is more accurate, the reaction is more sensitive, and the motion trajectory is smoother. It also can be seen that the fuzzy control algorithm reduces the actual distance that the master robot reaches the target position.

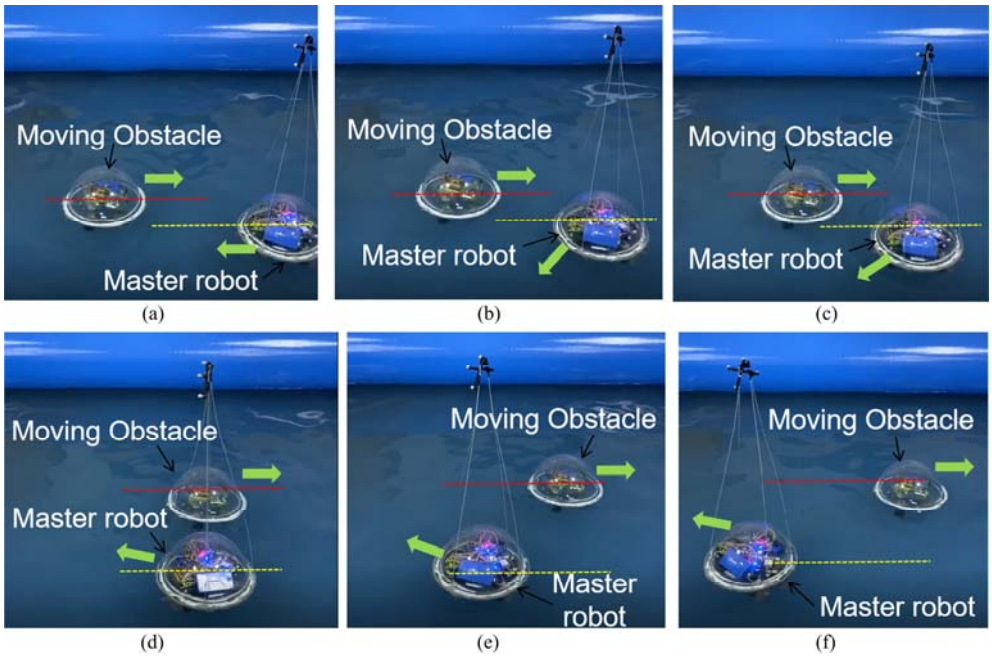

Fig. 12 Path planning experiments with moving obstacle in front. (a) t1; (b) t2; (c) t3; (d) t4; (e) t5; (f) t6.

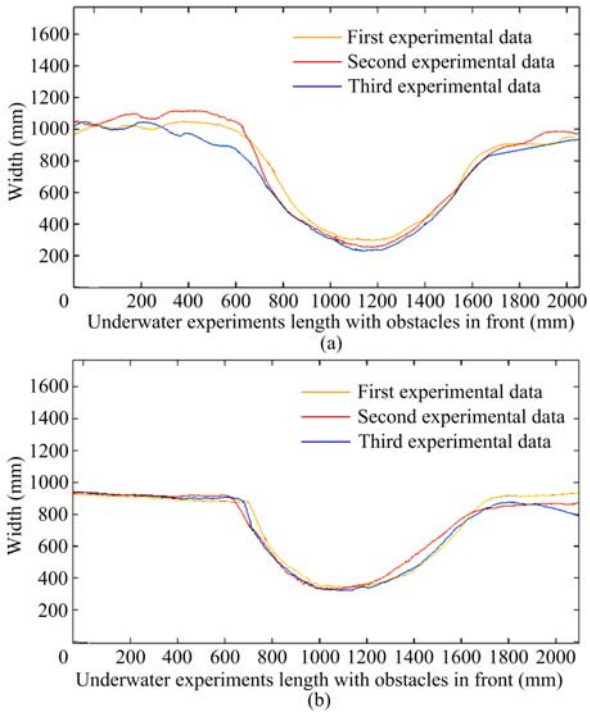

Fig. 13 The trajectory of the SUR with moving obstacle in front. (a) Experiments with basic control method; (b) experiments with novel fuzzy control method.

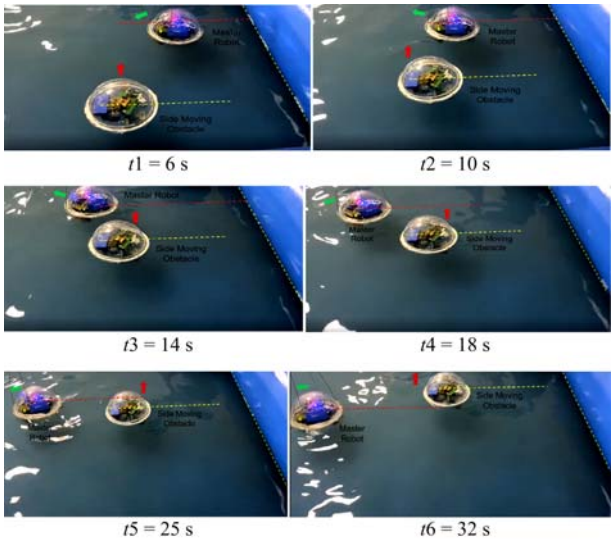

Fig. 14 Path planning experiments with moving obstacle on the side.

4.2 Path planning experiments with moving obstacle on the side

After completing the path planning experiments of the moving obstacles ahead, this paper also tested the obstacles on the side, and further verified the excellent performance of the fuzzy control algorithm. In the experiments with moving obstacles on the side, we used two SURs and set them as follows: the starting position of the robot is (300, 1200) and the target position is (1600, 380). And the obstacle is located on the left side of the master robot. The robot motion is shown in Fig. 14.

During the movement of the master robot, when the main robot detects an obstacle on the left side (t = 4 s), it starts to turn right to avoid obstacles. When avoiding the

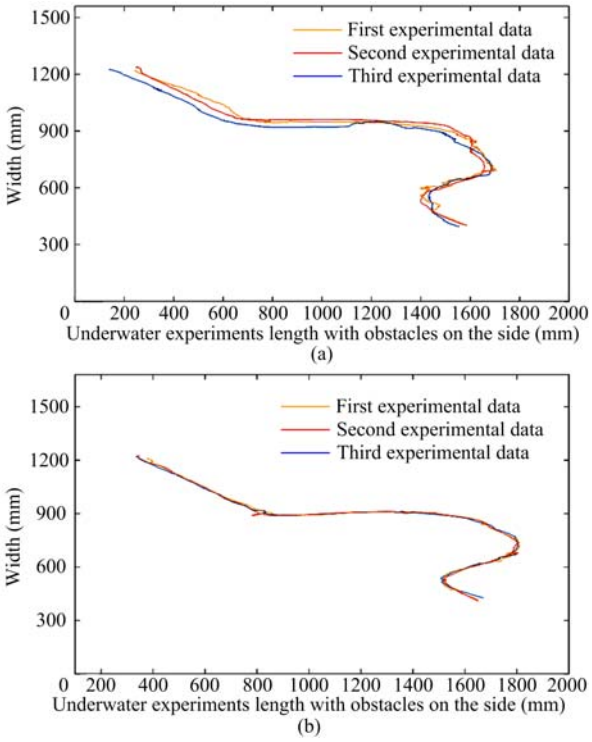

Fig. 15 The trajectory of the SUR with moving obstacle on the side. (a) Experiments with basic control method; (b) experiments with novel fuzzy control method.

obstacle, it starts to turn left and moves toward the target position (t = 8 s). Until the target position is reached.

We also compared the two experiments using the fuzzy control algorithm and with basic control method, as shown in Fig. 15. Each group of experiments ensures that the robot's motion speed, starting position and target position are the same.

It can be seen from Fig. 15 that the master robot with basic control method will have a jitter phenomenon during the motion, and the motion is unstable. Especially the jitter of motion trajectory in the obstacle avoidance process is serious. After adopting the fuzzy control algorithm, the motion trajectory has changed greatly, and the distance to reach the target position of the SUR has been shortened.

5 Discussion

When the SUR moves in the unknown water surface and underwater environments, the stability of the robot's movement is crucial for autonomous navigation and path planning. In order to effectively prove the effectiveness of the novel fuzzy control method, this paper guarantees that the starting position of the robot and the target position are same in the simulation and real environments. The same setting includes the number of sensors which is set to 4, the interval between sensors which is set to 60°, and the radius of robot is set to 15.5 cm, *etc*.

5.1 Evaluation of average time performance for the SUR

In the simulation experiments, as shown in Fig. 9 and Fig. 10, we set the same experimental parameters for each group, including the starting position, target position, and the movement speed of slave robot (the moving obstacle), the function of *SetTimeStep etc*, which ensure the reliability of the experiments. It can be seen from the Fig. 9a and Fig. 10a that when the robot adopts the basic control method, although the robot can safely reach the target position, during the movement, the robot's motion trajectory is unstable and it is difficult to move along the ideal trajectory. After adopting the novel fuzzy control method, as shown in Fig. 9b and Fig. 10b, the robot's motion is more stable, and the trajectory is almost the same every time, which guarantees the safe and reliable execution of tasks by the SUR. The parameter settings in the simulation experiments are shown in Table 3.

Next, this paper debugs the water jet motor to ensure that the thrust of four water jet motors remains the same in a real environment. This ensures the stable execution of the path planning experiment of the SUR. The thrust of the water jet thruster used in this paper is 0.2 N, and the input voltage is 9 V. After adopting the fuzzy control method, it can be seen from Fig. 13 and Fig. 15 that the SUR moves more stably, reduces the experimental error, and approaches the ideal trajectory.

The underwater experiments will still be disturbed by the external environment, which may cause the SUR to deviate from the ideal trajectory. This paper uses the following methods to deal with the interference of uncertain factors: Firstly, because water waves will affect the stability of the underwater robot, when the experiment is performed, this paper sets the robot's starting position and target position to be the same, also makes sure that the interval between experiments is certain to reduce the interference of water waves on the robot motion. Next, in order to ensure the accuracy of the path planning experiments in unknown environments, this

Table 3 Setting parameters for comparison experiments in simulation environments

Experiments	Algorithm	Initial position (m)	Target position (m)	Slave robot speed ($cm \cdot s^{-1}$)	SetTimeStep (s)
The moving obstacle in front	With basic control With fuzzy control	(0, 0.95)	(2.1, 0.95)	30	0.2
The moving obstacle on the side	With basic control With fuzzy control	(0.3, 1.2)	(1.6, 0.38)	30	0.2

Table 4 Setting parameters for comparison experiments in real environments

Experiments	Algorithm	Initial position (mm)	Target position (mm)	Sampling time (s)	Water jet thrust (N)	Average time (s)
The moving obstacle in front	With basic control	(0, 950)	(2100, 950)	40	0.2	38.3
	With fuzzy control					23.5
The moving obstacle on the side	With basic control	(300, 1200)	(1600, 380)	40	0.2	36.9
	With fuzzy control					23.6

paper uses NDI to track the robot trajectory with a measurement accuracy of 0.3 mm RMS.

Because the measurement range of NDI tracking system is limited, within 3.5 m, the measurement environment is limited. In order to more intuitively verify the performance of the fuzzy control algorithm, the average time of each group of experiments is calculated in this paper, as shown in Table 2. Due to the length of the actual distance is related to the time taken by the master robot to reach the target position, this paper guarantees that the starting position and target position of each group of experiments are consistent. Each group of experiments is tested three times, and the NDI tracking system is used to track the trajectory of the SUR. Each group of experiments verifies the effectiveness of the fuzzy control method by calculating the average time it takes for the robot to reach the target position.

It can be seen from Table 4 that the fuzzy control algorithm shortens the time it takes for the SUR to reach the target position by about 14 s. It can also be seen from the motion trajectory that the robot's response to obstacles is more sensitive, improving its self-adjust ability.

5.2 Evaluation of path travelled performance for the SUR

After analyzing the average time, this paper further calculated the path travelled of each experiment and analyzed the results. The path travelled is mainly reflected by the distance of the robot from the starting point to the target point.

The path travelled of the SUR in the simulation environment is shown in Fig. 16. Among them, the red-bar represents the straight-line distance from the starting point to the target point. The green-bar represents the path travelled using the basic control method. The yellow-bar represents the path travelled using the fuzzy control method. Fig. 16a is the path travelled when there is a moving obstacle in front, the ideal distance is 2100 mm. By calculating the average path travelled, the average travelled distance after using the basic control method is about 2300 mm, and the average path travelled after using the novel fuzzy control method is about 2180 mm. It can be seen that the path travelled is shortened by approximately 120 mm. Similarly, this paper also calculated the path travelled when there is a moving obstacle on the side, as shown in Fig. 16b, the ideal distance is 1430 mm. The path travelled after using the basic control method is about 1670 mm, and the average path travelled after using the novel fuzzy control method is about 1500 mm. It can be seen that the path travelled is shortened by approximately 170 mm.

The path travelled of the SUR in the real environment is shown in Fig. 17. The path travelled when there is a moving obstacle in front is shown in Fig. 17a, and the ideal distance is consistent with the simulation. The average path travelled after using the basic control method is about 2300 mm, and the average path travelled after using the novel fuzzy control method is about 2200 mm. It can be seen that the path travelled is shortened by approximately 100 mm. The path travelled when there is a moving obstacle on the side is shown in Fig. 17b, and the ideal distance is also consistent with the simulation. The average path travelled after using the basic control method is about 1750 mm, and the average

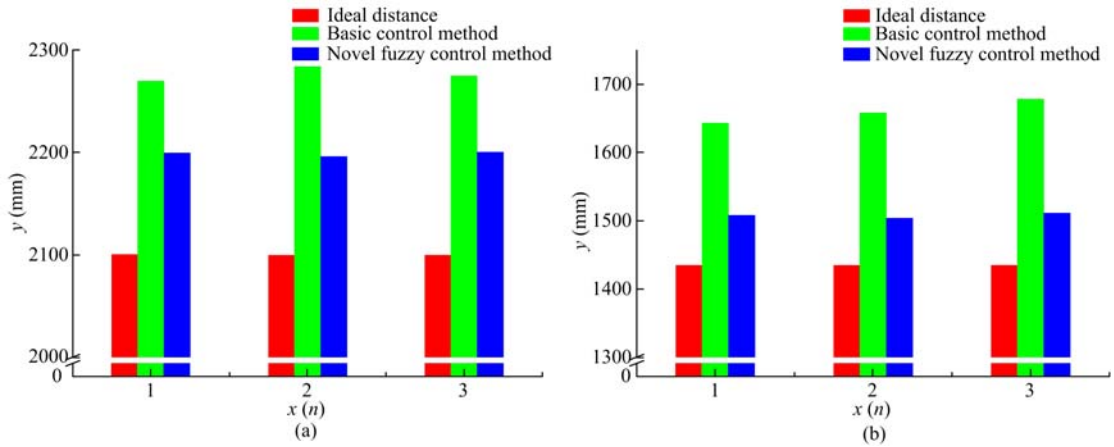

Fig. 16 Experimental result of the robot path travelled in simulation environment. (a) The moving obstacle in front; (b) the moving obstacle on the side.

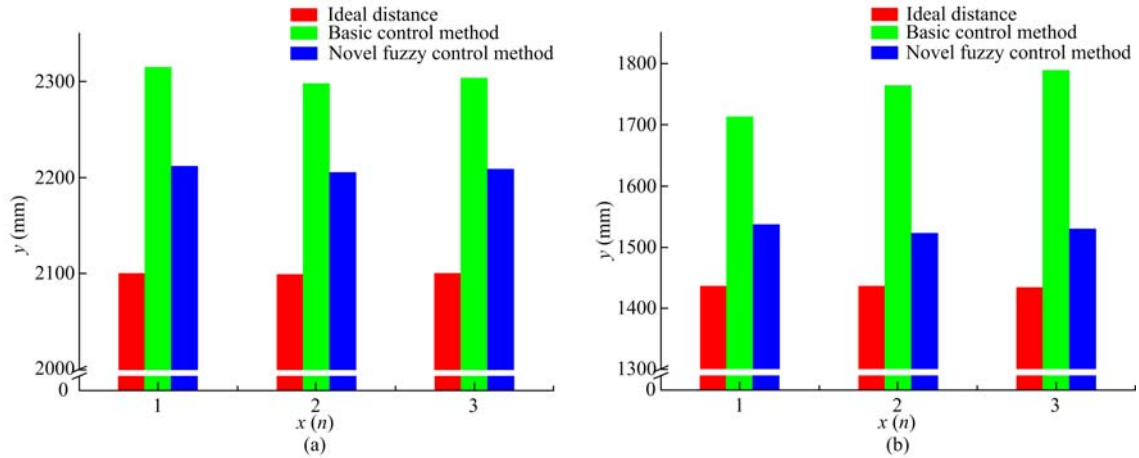

Fig. 17 Experimental result of the robot path travelled in real environment. (a) The moving obstacle in front; (b) the moving obstacle on the side.

path travelled after using the novel fuzzy control algorithm is about 1540 mm. It can be seen that the path travelled is shortened by approximately 210 mm.

In the real environment, due to the existence of certain external interference, the path of the SUR will have certain changes. However, it can be seen from the path planning experiments when there are the moving obstacle in front (Figs. 16a and 17a) and the moving obstacle on the side (Figs. 16b and 17b), the average path travelled is almost the same, which further validates the effectiveness and feasibility of the proposed method.

5.3 Evaluation of path deviation performance for the SUR

Finally, after carrying out the path planning experiments (simulation and real environment), this paper further analyzed the error, as shown in Fig. 18. Under the same conditions, the error also quickly converges and is adjusted by the controller. The error is stable between 0 m and 0.1 m, and the error is small. In the experiments under simulation and real environment, there are still some deviations. The main reason is that the robot will be subject to certain external interference in the underwater environment, and the system will appear corresponding jitter, but the overall error does not exceed 5%, which meets the actual requirements of the engineering. Therefore, the error analysis experiment further proves the feasibility and effectiveness of the proposed method.

The novel fuzzy control method used in this paper not only improves the flexibility of the SUR, but also optimizes the time and distance for the robot to reach the target position, and the motion trajectory is smoother. This will ensure the execution efficiency of the SUR in unknown environments.

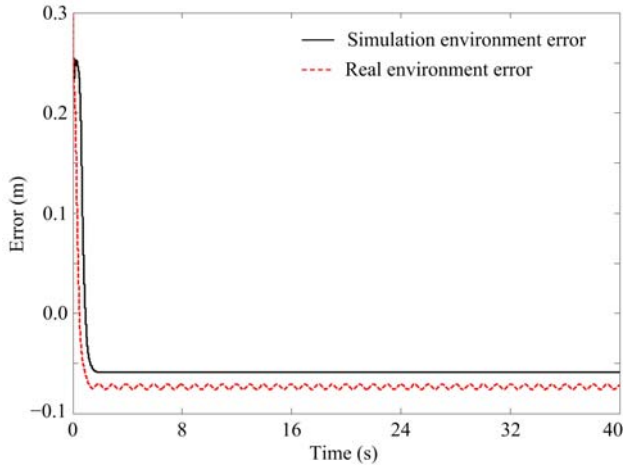

Fig. 18 The error in path planning experiments (Simulation and real environment).

6 Conclusion and future work

To improve the autonomous navigation of the SUR in the unknown environment, this paper proposed a path planning method for the SUR based on fuzzy control. Firstly, by analyzing the kinematic model of the SUR, this paper completed the arrangement of the ultrasonic sensors (US1000-21A), and calculated the minimum safety distance. This paper, then, designed the fuzzy controller using Matlab Fuzzy Toolbox, and constructed the good control response table, and also carried out simulation experiments in an unknown environment. Next, a series of underwater path planning experiments were performed in this paper using ultrasonic sensors. The scenario of the path planning experiments were as follows: Scenario 1, with moving obstacle in front; Scenario 2, with moving obstacle on the side. Finally, this paper completed comparative experiments that with using fuzzy control method and basic control method, and analyzed the experimental results by calculating the average time.

The experimental results showed that the fuzzy control method met the autonomous navigation requirements of the SUR in unknown environments, and verified the effectiveness and feasibility of the fuzzy control system. In the future, we will use the SUR to complete experiments in deep water.

Acknowledgement

This work was supported in part by the National Natural Science Foundation of China (Grant No. 61703305), in part by the Key Research Program of the Natural Science Foundation of Tianjin (Grant No. 18JCZDJC38500), and in part by the Innovative Cooperation Project of Tianjin Scientific and Technological (Grant No. 18PTZWHZ00090).

References

[1] Xian Z W, He X F, Lian J X, Hu X P, Zhang L L. A bionic autonomous navigation system by using polarization navigation sensor and stereo camera. *Autonomous Robots*, 2017, **41**, 1107–1118.

[2] Francisco B F, Miquel M C, Pep L N C, Gabriel O C, Joan P B. Inertial sensor self-calibration in a visually-aided navigation approach for a micro-AUV. *Sensors*, 2015, **15**, 1825–1860.

[3] Kularatne D, Bhattacharya S, Hsieh M A. Going with the flow: A graph based approach to optimal path planning in general flows. *Autonomous Robots*, 2018, **42**, 1369–1387.

[4] Zhang Z J, Chen S Y, Li S. Compatible convex-nonconvex constrained QP-based dual neural networks for motion planning of redundant robot manipulators. *IEEE Transactions on Control Systems Technology*, 2019, **27**, 1250–1258.

[5] Ji J, Khajepour A, Melek W W, Huang Y J. Path planning and tracking for vehicle collision avoidance based on model predictive control with multiconstraints. *IEEE Transactions on Vehicular Technology*, 2017, **66**, 952–964.

[6] Han Y Q, Kao Y G, Gao C C. Robust sliding mode control for uncertain discrete singular systems with time-varying delays and external disturbances. *Automatica*, 2017, **75**, 210–216.

[7] Ma Y N, Gong Y J, Xiao C F, Gao Y. Path planning for autonomous underwater vehicles: An ant colony algorithm incorporating alarm pheromone. *IEEE Transactions on Vehicular Technology*, 2019, **68**, 141–154.

[8] Duan Q J, Zhang M J, Zhang J. Local path planning method for AUV based on fuzzy-neural network. *Ship Engineering*, 2001, 54–58. (in Chinese)

[9] Duan Q J, Zhang M J. Research on real time path planning method for the underwater robot in unknown environment with random shape obstacle. *IEEE International Conference on Mechatronics & Automation*, *ICMA*, Luoyang, China, 2006, 757–761.

[10] Chen M J, Lin W, Zeng B. Path planning for robot autonomous map building based on rolling window. *Computer Engineering*, 2017, **43**, 286–292. (in Chinese)

[11] Chen J W, Zhu H C, Zhang L, Sun Y X. Research on fuzzy control of path tracking for underwater vehicle based on

genetic algorithm optimization. *Ocean Engineering*, 2018, **156**, 217–223.

[12] Guo J, Li C Y, Guo S X. Study on the path planning of the spherical mobile robot based on fuzzy control. *IEEE International Conference on Mechatronics and Automation*, *ICMA*, Tianjin, China, 2019, 1419–1424.

[13] Shi L W, Guo S X, Mao S L, Yue C F, Li M X, Asaka K J. Development of an amphibious turtle-inspired, spherical mother robot. *Journal of Bionic Engineering*, 2013, **10**, 446–455.

[14] Guo S X, He Y L, Shi L W, Pan S W, Xiao R, Tang K, Guo P. Modeling and experimental evaluation of an improved amphibious robot with compact structure. *Robot and Computer-Integrated Manufacturing*, 2018, **51**, 37–52.

[15] Xing H M, Shi L W, Tang K, Guo S X, Hou X H, Liu Y, Liu H K, Hu Y. Robust RGB-D camera and IMU fusion-based cooperative and relative close-range localization for multiple turtle-inspired amphibious spherical robots. *Journal of Bionic Engineering*, 2019, **16**, 442–454.

[16] Guo J, Li C Y, Guo S X. A novel step optimal path planning algorithm for the spherical mobile robot based on fuzzy control. *IEEE Access*, 2020, **8**, 1394–1405.

[17] Gan W Y, Zhu D Q, Sun B, Luo C M. The tracking control of unmanned underwater vehicles based on QPSO-model predictive control. *International Conference on Intelligent Robotics and Applications*, *ICIRA*, Wuhan, China, 2017, 711–720.

[18] Salumae T, Chemori A, Kruusmaa M. Motion control of a hovering biomimetic four-fin underwater robot. *IEEE Journal of Oceanic Engineering*, 2019, **44**, 54–71.

[19] Kim H, Lee J. Design, swimming motion planning and implementation of a legged underwater robot (CALEB10: D.BeeBot) by biomimetic approach. *Ocean Engineering*, 2017, **130**, 310–327.

[20] Guo S X, Yang X J, Guo J. Study on horizontal path tracking control method for the spherical amphibious robot. *IEEE International Conference on Mechatronics and Automation*, *ICMA*, Tianjin, China, 2019, 1155–1160.

[21] Singh V, Willcox K E. Methodology for path planning with dynamic data-driven flight capability estimation. *AIAA Journal*, 2017, **55**, 2727–2738.

[22] Rao D C, Kabat M R, Das P K, Jena P K. Hybrid IWD-DE: A novel approach to model cooperative navigation planning for multi-robot in unknown dynamic environment. *Journal of Bionic Engineering*, 2019, **16**, 235–252.

[23] Michalopoulou Z H, Abdi A. Detection in an uncertain underwater waveguide. *Journal of the Acoustical Society of America*, 2017, **142**, 2553–2553.

[24] Liu J K. *Robot Control System Design and MATLAB Simulation the Advanced Design Method*, Tsinghua University Press, Beijing, China, 2017. (in Chinese)

[25] Halin H, Khairunizam W, Ikram K, Haris H, Zunaidi I, Bakar S A, Razlan Z M, Desa H. Design simulation of a fuzzy steering wheel controller for a buggy car. *International Conference on Intelligent Informatics & Biomedical Sciences IEEE Computer Society*, 2018, **3**, 85–89.